THE JOURNAL OF PHYSICAL CHEMISTRY C

Letter

Density Functional Theory of in Situ Synchrotron Powder X-ray Diffraction on Mesoporous Crystals: Argon Adsorption on MCM-41

Keiichi Miyasaka, Alexander V. Neimark, and Osamu Terasaki

J. Phys. Chem. C, **2009**, 113 (3), 791-794• DOI: 10.1021/jp810368h • Publication Date (Web): 22 December 2008

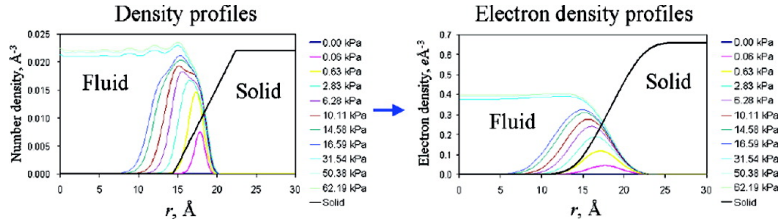

More About This Article

Additional resources and features associated with this article are available within the HTML version:

- Supporting Information
- Access to high resolution figures
- Links to articles and content related to this article
- Copyright permission to reproduce figures and/or text from this article

View the Full Text HTML

THE JOURNAL OF PHYSICAL CHEMISTRY C LETTERS

2009, *113,* 791–794
Published on Web 12/22/2008

Density Functional Theory of in Situ Synchrotron Powder X-ray Diffraction on Mesoporous Crystals: Argon Adsorption on MCM-41

Keiichi Miyasaka,*,† Alexander V. Neimark,*,‡ and Osamu Terasaki†

Structural Chemistry, Arrhenius Laboratory, Stockholm University, SE-10691 Stockholm, Sweden, and Department of Chemical and Biochemical Engineering, Rutgers, The State University of New Jersey, 98 Brett Road, Piscataway, New Jersey 08854-8058

Received: November 25, 2008

The process of gas adsorption on mesoporous crystals can be explored by in situ synchrotron powder X-ray diffraction (XRD) that provides direct information about the distribution of adsorbate with the pore channels. We presented a rigorous theoretical framework for interpretation of the in situ XRD data based on the novel quenched solid density functional theory (QSDFT) model of adsorption on mesoporous materials. QSDFT accounts for the molecular level roughness of the pore walls that is shown to be one of the major factors affecting both the adsorption isotherms and the XRD patterns. Drawing on the example of Ar adsorption in pores of MCM-41, we demonstrate that, using the intermolecular potentials established from the adsorption data and the structural parameters (pore size and roughness) determined from the XRD data, the QSDFT model describes the in situ synchrotron powder XRD intensities on a quantitative level. The QSDFT model provides an opportunity for a unified interpretation of adsorption and XRD measurements on mesoporous materials reconciling these two independent experimental methods widely employed for pore structure characterization. Combined with QSDFT, in situ synchrotron XRD measurements offer a powerful tool for studies of the specifics of adsorption mechanisms and phase transformations in nanoconfined fluids.

Since their discovery in the early 1990s, ordered mesoporous silicas[1−3] have been recognized as promising materials for various applications due to their uniform pore structure, which can be tailored and fine-tuned during synthesis to meet desired engineering requirements.[4] Mesoporous silicas, such as MCM-41, represent ordered pore networks embedded in amorphous solid matrix. These materials may be called "mesoporous crystals", since they exhibit a clear crystallographic symmetry revealed in scattering experiments. A better understanding of the process of gas adsorption onto the mesopores is crucial for the optimal design of novel adsorbents, catalysts, and separation membranes. The process of gas adsorption on mesoporous crystals can be explored by in situ powder X-ray diffraction (XRD) that has recently attracted considerable attention.[5−9] This technique provides direct information about the distribution of adsorbate, which is concentrated only around the reciprocal lattice points due to the periodicity of the mesoporous crystals. However, the structure of mesoporous crystals, which originates from soft matter mesophases, is subject to significant heterogeneities and variations compared to ordinary solid crystals. There are several factors contributing to structural deviations: (i) the solid matrix is amorphous and the pore wall surface is intrinsically rough on the atomic scale; (ii) pore channels vary in diameter and their shape may be corrugated; (iii) positions of pores fluctuate around the sites of the crystallographic lattice; (iv) the solid matrix may be microporous[5] and its density may be reduced compared with the density of amorphous silica. In the case of MCM-41 mesoporous crystals with two-dimensional (2D) *p6mm* symmetry, it is reasonable to treat pores as cylindrical channels, with positions and diameters that are averaged over the lattice sites and along the channel direction. Such coarse-grained representation of mesoporous crystals should reflect their inherent heterogeneous features. Various models that take into account the surface roughness, lattice fluctuations, and thermal vibrations have already been employed in the literature for analyzing XRD data on mesoporous crystals.[10−14]

Gas adsorption is a traditional technique and is extensively used for characterization of porous solids. It provides information about porosity, surface area, and pore sizes independently from XRD experiments.[15] Among a variety of theoretical methods, density functional theory (DFT) has been perceived as a powerful technique for interpretation of adsorption isotherms.[16] The nonlocal density functional theory (NLDFT) models were developed for characterization of mesoporous silica crystals with different symmetries,[17−19] which allows one not only to calculate the pore size distribution but also to discriminate between different structures with the same space group symmetry.[20] Recently, the NLDFT model has been extended to account for the surface roughness and matrix microporosity in the form of so-called quenched solid density functional theory (QSDFT).[21] The QSDFT operates with both adsorbate (fluid) and adsorbent (solid) densities in contrast with the conventional DFT models, which assume ideal and molecularly smooth pore walls.[22] The solid density distribution employed within QSDFT reflects the surface roughness and possible microporosity. The

* Corresponding authors. E-mail: aneimark@rutgers.edu (A.V.N.); kei@struc.su.se (K.M.).
† Stockholm University.
‡ Rutgers, The State University of New Jersey.

10.1021/jp810368h CCC: $40.75

QSDFT model enables one to calculate at given environmental conditions of gas pressure and temperature the equilibrium fluid density profiles (DPs) in model pores of simple morphologies (slits, cylinders, and spheres) confined by solid walls with given distributions of solid density introduced as quenched solid DPs. The QSDFT model was shown to adequately describe adsorption of cryogenic gases on nonporous and mesoporous silicas.[21] In our previous publication,[9] we demonstrated that the QSDFT model was instrumental in the interpretation of adsorption isotherms measured in in situ synchrotron powder XRD experiments for Ar adsorption on a typical 2D hexagonal ordered mesoporous crystal MCM-41.

In the present paper, we extend the QSDFT model for calculating not only the adsorption isotherms but also the reflection intensities measured during the adsorption of Ar on MCM-41 in a wide range of gas pressures at a constant temperature.[9] It is worth noting that the sample temperature in the in situ XRD experiments cannot be measured directly.[9] The test tube with the sample is cooled by a jet of evaporating liquid nitrogen, so that the sample temperature, which depends on the heat exchange conditions, may vary between the boiling temperatures of the cooling agent (77.4 K) and the adsorbate (87.3 K). Since the adsorption process is very sensitive to even minor variations of temperature, the determination of the sample temperature is a necessary step in the theoretical description of adsorption. The approach presented below is straightforward. First, we determine the geometrical parameters of the QSDFT model for the sample under consideration. These parameters, the mean pore diameter D and the surface roughness parameter δ, are calculated from the solid profiles obtained from the XRD data for two measurements with the dry (the pressure = 0 kPa) and the wet (completely saturated) samples. Second, we calculate with the QSDFT model the Ar adsorption isotherms at different temperatures and determine the sample temperature T by fitting the calculated isotherm to the experimental one. Third, we calculate the adsorbate DPs with the QSDFT model at this temperature T for a set of gas pressures corresponding to the in situ XRD measurements and convert the DPs into the electron density profiles (EDPs) needed for simulating the XRD intensity. Forth, we calculate the XRD intensities by applying the Fourier transform to the combination of solid and fluid EDPs.

In general, a crystal structure can be described as the convolution of the basis $b(\mathbf{r})$ and the lattice $l(\mathbf{r})$ functions

$$c(\mathbf{r}) = b(\mathbf{r}) * l(\mathbf{r}) = \int \mathrm{d}\mathbf{r}'\, b(\mathbf{r}-\mathbf{r}')l(\mathbf{r}') \qquad (1)$$

Fourier transform (designated as F) of $c(\mathbf{r})$ represents the crystal structure factor $C(\mathbf{k}) = B(\mathbf{k})\cdot L(\mathbf{k})$, where $\mathbf{k}$ is the wavenumber vector, $B(\mathbf{k}) = F[b(\mathbf{r})]$ and $L(\mathbf{k}) = F[l(\mathbf{r})]$. Here, $l(\mathbf{r})$ reflects the 2D hexagonal lattice symmetry of the MCM-41 crystal, whereas $b(\mathbf{r})$ reflects the cylindrical symmetry of individual pore channels, and it is assumed to be dependent only on the radial coordinate r. Possible fluctuations of density along the pore channel are implicitly accounted by the mean solid DP, which includes averaging over both angular and longitudinal coordinates. The basis $b(\mathbf{r})$ is constructed from the given solid DP and the fluid DP calculated by QSDFT. Then, the combined DP as the crystallographic basis can be expressed as

$$b_{\mathrm{DP}}(r) = \rho_{\mathrm{solid}} - b_{\mathrm{pore}}(r) + b_{\mathrm{fluid}}(r) \qquad (2)$$

where $\rho_{\mathrm{solid}} = 0.022$ Å^{-3} is the constant number density of the SiO_2 unit (based on the presumed silica wall density of 2.2 g/cm^3), $b_{\mathrm{pore}}(r)$ is the "pore" density profile, and thus $\rho_{\mathrm{solid}} - b_{\mathrm{pore}}(r)$ complementarily represents the given DP of the silica wall involving its surface roughness within the QSDFT scheme.

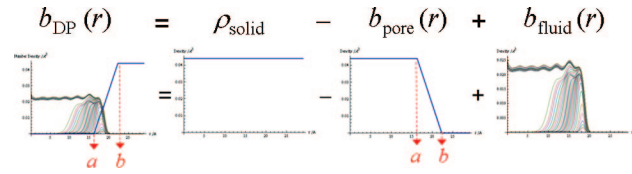

Figure 1. Schematics for the solid and fluid density profiles along the pore radial coordinate. The combined density profile ($b_{\mathrm{DP}}(r)$) of fluid and solid is composed of the mesopore pore wall density profile ($\rho_{\mathrm{solid}} - b_{\mathrm{pore}}(r)$) and the simulated fluid density profile ($b_{\mathrm{fluid}}(r)$). The density profile $b_{\mathrm{pore}}(r)$ describes the surface roughness; a and b are the inner and outer boundaries of the linear ramp, respectively, $b - a = 2\delta$.

$b_{\mathrm{fluid}}(r)$ is the fluid DP calculated by QSDFT. We approximated the solid DP as a linear ramp, and its semiwidth represents the roughness parameter δ, see Figure 1. Although other approximations to the solid DP may be more realistic in molecular dynamics simulation for amorphous silica surfaces,[23] the linear ramp profile was previously reported to give an adequate description of the experimental data of Ar adsorption on MCM-41 material.[21]

In order to simulate XRD intensity, we need to convert DP to the corresponding EDP. This can be done by convolving the kernel $\varepsilon(\mathbf{r})$ representing the electron cloud with the distribution of atomic centers $b(r)$, which is expressed as $\varepsilon * b(\mathbf{r})$. Thereby the function $b_{\mathrm{DP}}(r)$ for the density of the centers of relevant atoms can be transformed into the associated EDP through

$$b_{\mathrm{EDP}}(r) = \varepsilon_{\mathrm{solid}}(\rho_{\mathrm{solid}} - b_{\mathrm{pore}})(r) + \varepsilon_{\mathrm{fluid}} b_{\mathrm{fluid}}(r) \qquad (3)$$

where $\varepsilon_{\mathrm{solid}}$ and $\varepsilon_{\mathrm{fluid}}$ represent an electron spread around the solid and fluid molecules, respectively. The Fourier transform of $b_{\mathrm{EDP}}(r)$ gives the scattering factor, reading as

$$\begin{aligned} B_{\mathrm{EDP}}(k) &= E_{\mathrm{solid}}(k)\cdot\{\rho_{\mathrm{solid}}\delta(k) - B_{\mathrm{pore}}(k)\} + E_{\mathrm{fluid}}(k)\cdot B_{\mathrm{fluid}}(k) \\ &= -E_{\mathrm{solid}}(k)\cdot B_{\mathrm{pore}}(k) + E_{\mathrm{fluid}}(k)\cdot B_{\mathrm{fluid}}(k) \qquad \text{when } k \neq 0 \end{aligned} \qquad (4)$$

where k is the length of $\mathbf{k}$, $E_{\mathrm{solid}} = F[\varepsilon_{\mathrm{solid}}(\mathbf{r})]$, $B_{\mathrm{pore}} = F[b_{\mathrm{pore}}(\mathbf{r})]$, $E_{\mathrm{fluid}} = F[\varepsilon_{\mathrm{fluid}}(\mathbf{r})]$, and $B_{\mathrm{fluid}} = F[b_{\mathrm{fluid}}(\mathbf{r})]$, respectively. k of the 2D hexagonal lattice is associated with a reflection indexed by HK via

$$k_{hk} = \frac{2}{a_c}\sqrt{\frac{H^2 + K^2 + HK}{3}} \qquad (5)$$

where a_c denotes the cell parameter equal to the distance between the centers of neighboring mesopores. Accordingly, the diffraction intensity based on the structure factor of HK reflection is given by $I_{HK} = |B_{\mathrm{EDP}}(k_{HK})|^2$. To compare it with the intensities observed in powder XRD, other factors affecting the intensity need to be corrected, see below.

Fourier transform for cylindrical objects was early derived by Oster and Riley.[24] The "pore" density profile with the linear ramp, $B_{\mathrm{pore}}(k)$, is Fourier transformed as

$$\begin{aligned} B_{\mathrm{pore}}(k) = {} & \frac{1}{k(b-a)}[b^2 J_1(2\pi bk) - a^2 J_1(2\pi ak)] + \\ & \frac{2}{3\pi(b-a)}\left[b^3\,{}_1F_2\left(\frac{3}{2};1,\frac{5}{2};\pi^2b^2k^2\right) - a^3\,{}_1F_2\left(\frac{3}{2};1,\frac{5}{2};\pi^2a^2k^2\right)\right] \end{aligned} \qquad (6)$$

where J_1 is the Bessel function with the first order, and ${}_1F_2$ is the hypergeometric function. The Fourier transform of the fluid DP $B_{\mathrm{fluid}}(k)$ is calculated numerically at every pressure.

The DP of QSDFT represents a probability distribution of atomic centers of adsorbed molecules, which is equivalent to the overall mean density distribution of Ar atoms. For both solid

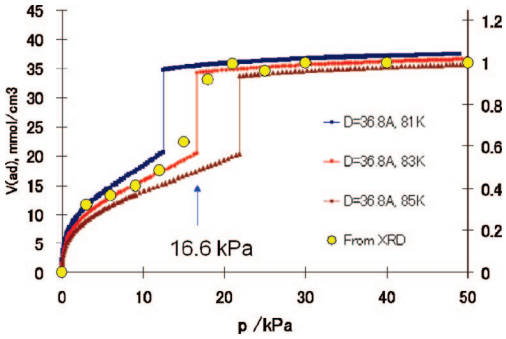

Figure 2. Based on the cylindrical geometry of MCM-41 mesoporous crystal with the mean pore diameter of 36.8 Å and the surface roughness of 4 Å, the theoretical isotherms predicted by QSDFT model at different temperatures (81, 83, and 85 K) are compared with the isotherm estimated from the in situ powder XRD data. The left vertical axis (for QSDFT data) represents the theoretical amount of Ar adsorbed, and the right axis (for XRD data) is the volume of gas film relative to the empty pore volume at "dry" condition (pressure = 0 kPa).

and fluid, the homogeneous electron spreads ε_{solid} and ε_{fluid} are introduced as Gaussian functions

$$\varepsilon(|\mathbf{r}|) = N_e(2\pi\sigma^2)^{-3/2}\exp[-|\mathbf{r}|^2/2\sigma^2] \quad (7)$$

where N_e denotes the number of electrons and σ is related to the half-width of the electron spread. Its Fourier transform with cylindrical isotropy becomes

$$E(|\mathbf{k}|) = N_e\exp[-2\pi^2\sigma^2|\mathbf{k}|^2] \quad (8)$$

Here, σ has been set as the Van der Waals radius for each atom, i.e. O (1.52 Å), Si (2.1 Å), and Ar (1.88 Å). Different types of electron spreads other than a single Gaussian function, e.g., five Gaussian terms,[25] were also tested; it was shown that they made insignificant differences.

The geometrical parameters of the wall density distribution required for QSDFT calculations, were taken from our in situ XRD experiment reported early in ref 9: the cell parameter a_c = 44.8 Å, the mean pore diameter D = 36.8 Å, and the surface roughness parameter δ = 4 Å. To determine the sample temperature in in situ XRD experiments, we calculated equilibrium isotherms of Ar adsorption at different temperatures. These isotherms were compared with the isotherm estimated from the XRD data, see Figure 2. We found that the temperature of 83K provided the best fit of the theoretical isotherm to the experimental data. Thus, we concluded that the sample temperature in the in situ XRD measurements should be taken as 83 K. We have to acknowledge that this temperature is somewhat different from that of 81 K estimated in ref 9. This difference originates in the difference of the mean pore diameters used for the QSDFT calculations. In ref 9, the pore diameter of 42 Å was defined from the adsorption isotherm measured at 87.3 K by using the NLDFT method.[17] In this work, we rely upon the in situ XRD data on the pore diameter, and we do not invoke the adsorption measurements at all.

On the basis of the determined parameters (D = 36.8 Å, δ = 4 Å, and T = 83 K), the DPs for Ar gas have been simulated by QSDFT. They are shown in Figure 3 together with the EDPs converted with the Gaussian electron cloud. The mean positions of the solid and fluid boundaries are not changed by this conversion, while the steps of the EDPs become smoother than those of the DPs because of the convolution operation. The experimental XRD gave 10, 11, and 20 reflections at every pressure ranging from 0 to 50 kPa.[9] The wavenumbers are k_{10} = 0.026 Å^{-1}, k_{11} = 0.045 Å^{-1}, and k_{20} = 0.052 Å^{-1},

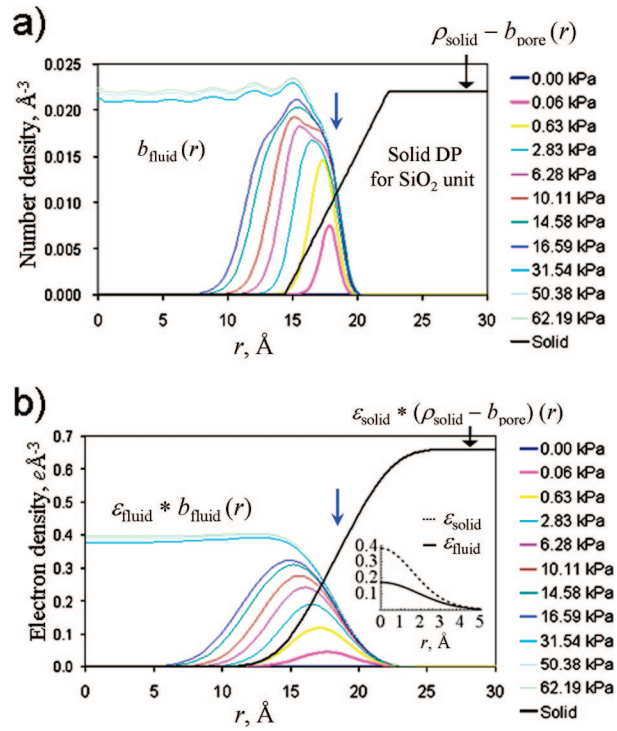

Figure 3. (a) Prescribed solid DP for amorphous silica and the calculated DPs by QSDFT. (b) The corresponding EDPs converted from the DPs in (a). The conversion was done by convolution with the Gaussian kernel of the electron spread of solid and fluid (inset). Blue arrows indicate the position of the mean pore radius, 18.4 Å.

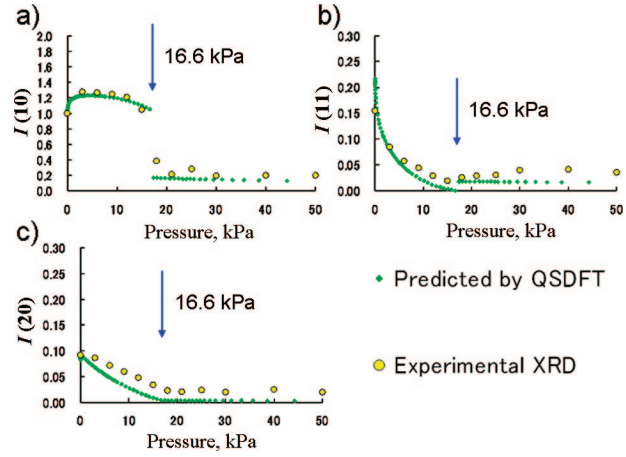

Figure 4. Comparison of the theoretical diffraction intensities calculated from DPs of QSDFT and the experimental diffraction intensities measured during in situ powder XRD[9] for Ar adsorption on MCM-41 mesoporous crystal. (a) 10, (b) 11, and (c) 20 reflections are presented. The capillary condensation is considered to take place at 16.6 kPa on condition of T = 83 K.

respectively, according to Eq (5). In addition to the structure factor, the observed powder XRD intensities are affected also by Lorentz, polarization, absorption, temperature, and multiplicity factors. These factors are compensated so that I_{HK} calculated from the DPs of QSDFT is comparable with the corresponding experimental data. The comparison between the QSDFT prediction and the experimental observation is shown in Figure 4, where the intensities I_{HK} are normalized using I_{10} at "dry" condition (0 kPa). The plots show quantitative agreement between the theoretical and experimental intensities as the functions of the increasing gas pressure. It should be pointed out that QSDFT has accurately predicted XRD intensities not

only of the main 10 reflection but also of the other 11 and 20 reflections. Deviations between QSDFT and XRD data on I_{11} and I_{20} intensities are more pronounced at higher pressures. At the "dry" condition, the diffraction intensities are determined by the geometrical factors used in QSDFT (D and δ). When the sample is partially "wet", the system becomes more intricate and the contributions from additional factors such as the ratio of solid and fluid densities and the variations from the assumed cylindrical symmetry, may affect the experimental intensities. The QSDFT assumes the simplest geometrical model with just two geometrical parameters, and the fact that this "minimal" semiquantitatively describes in a unified manner both adsorption and XRD processes is noteworthy.

In conclusions, we presented a rigorous theoretical framework for calculating the diffraction intensities during in situ synchrotron powder XRD measurements of gas adsorption on mesoporous crystals. Drawing on the example of Ar adsorption on MCM-41 silica, we showed that based on the structural parameters revealed from the XRD experiments with dry and wet samples, it was possible to semiquantitatively predict the diffraction intensity data measured during the adsorption process. The key steps in the proposed methods include the calculation of the adsorbate DP at given gas pressure by using the QSDFT model, the conversion of the calculated DP into the respective EDP, and the Fourier transform of the EDP that gives the theoretical diffraction intensities. Good agreement of theoretical and experimental diffraction intensities suggests that the QSDFT model grasps the main features of the gas adsorption process on molecularly rough surfaces of ordered mesoporous solids. The QSDFT model provides an opportunity for a unified interpretation of adsorption and XRD measurements of mesoporous materials reconciling these two independent experimental methods widely employed for pore structure characterization. Combined with QSDFT, in situ synchrotron XRD measurements offer a powerful tool for studies of the specifics of adsorption mechanisms and phase transformations in nanoconfined fluids.

Acknowledgment. The authors thank Drs. Muroyama and Ravikovitch for fruitful discussions and help with analyses of experimental results and computations given in ref 9. O.T. thanks Swedish Research Council (VR) and Japanese Science and Technology Agency (JST) for financial support. A.V.N. acknowledges partial support from NSF ERC "Structured Organic Particulate Systems" and Quantachrome Instruments.

References and Notes

(1) Yanagisawa, T.; Shimizu, T.; Kuroda, K.; Kato, C. *Bull. Chem. Soc. Jpn.* **1990**, *63*, 988.
(2) Kresge, C. T.; Leonowicz, M. E.; Roth, W. J.; Vartuli, J. C.; Beck, J. S. *Nature* **1992**, *359*, 710.
(3) Beck, J. S.; Vartuli, J. C.; Roth, W. J.; Leonowicz, M. E.; Kresge, C. T.; Schmitt, K. D.; Chu, C. T. W.; Olson, D. H.; Sheppard, E. W.; Mccullen, S. B.; Higgins, J. B.; Schlenker, J. L. *J. Am. Chem. Soc.* **1992**, *114*, 10834.
(4) Wan, Y.; Zhao, D. Y. *Chem. Rev.* **2007**, *107*, 2821.
(5) Albouy, P. A.; Ayral, A. *Chem. Mater.* **2002**, *14*, 3391.
(6) Hofmann, T.; Wallacher, D.; Huber, P.; Birringer, R.; Knorr, K.; Schreiber, A.; Findenegg, G. H. *Phys. Rev. B* **2005**, *72*, 064122.
(7) Zickler, G. A.; Jahnert, S.; Wagermaier, W.; Funari, S. S.; Findenegg, G. H.; Paris, O. *Phys. Rev. B* **2006**, *73*, 184109.
(8) Zickler, G. A.; Jahnert, S.; Funari, S. S.; Findenegg, G. H.; Paris, O. *J. Appl. Crystallogr.* **2007**, *40* (Supplement), s522.
(9) Muroyama, N.; Yoshimura, A.; Kubota, Y.; Miyasaka, K.; Ohsuna, T.; Ryoo, R.; Ravikovitch, P.; Neimark, A.; Takata, M.; Terasaki, O. *J. Phys. Chem. C* **2008**, *112*, 10803.
(10) Tun, Z.; Mason, P. C. *Acta Crystallogr., Sect. A* **2000**, *56*, 536.
(11) Imperor-Clerc, M.; Davidson, P.; Davidson, A. *J. Am. Chem. Soc.* **2000**, *122*, 11925.
(12) Fenelonov, V. B.; Derevyankin, A. Y.; Kirik, S. D.; Solovyov, L. A.; Shmakov, A. N.; Bonardet, J. L.; Gedeon, A.; Romannikov, V. N. *Microporous Mesoporous Mater.* **2001**, *44*, 33.
(13) Sauer, J.; Marlow, F.; Schuth, F. *Phys. Chem. Chem. Phys.* **2001**, *3*, 5579.
(14) Muroyama, N.; Ohsuna, T.; Ryoo, R.; Kubota, Y.; Terasaki, O. *J. Phys. Chem. B* **2006**, *110*, 10630.
(15) Gregg, S. J.; Sing, K. S. W. *Adsorption, Surface Area, and Porosity*; Academic Press: London, U.K., 1982.
(16) Wu, J. Z. *AIChE J.* **2006**, *52*, 1169.
(17) Neimark, A. V.; Ravikovitch, P. I.; Grun, M.; Schuth, F.; Unger, K. K. *J. Colloid Interface Sci.* **1998**, *207*, 159.
(18) Schumacher, K.; Ravikovitch, P. I.; Du Chesne, A.; Neimark, A. V.; Unger, K. K. *Langmuir* **2000**, *16*, 4648.
(19) Ravikovitch, P. I.; Neimark, A. V. *Langmuir* **2002**, *18*, 1550.
(20) Ravikovitch, P. I.; Neimark, A. V. *Langmuir* **2000**, *16*, 2419.
(21) Ravikovitch, P. I.; Neimark, A. V. *Langmuir* **2006**, *22*, 11171.
(22) Olivier, J. P. *Carbon* **1998**, *36*, 1469.
(23) Rarivomanantsoa, M.; Jund, P.; Jullien, R. *J. Phys.-Condens. Matter* **2001**, *13*, 6707.
(24) Oster, G.; Riley, D. P. *Acta Crystallogr.* **1952**, *5*, 272.
(25) Waasmaier, D.; Kirfel, A. *Acta Crystallogr., Sect. A* **1995**, *51*, 416.

JP810368H